

A Physically-Based Electron Mobility Model for Strained Si Devices

S. Dhar, H. Kosina, V. Palankovski, E. Ungersboeck, and S. Selberherr

Institute for Microelectronics, Vienna University of Technology
Gusshausstrasse 27–29, A–1040 Vienna, Austria, dhar@iue.tuwien.ac.at

ABSTRACT

A model describing the mobility tensor for electrons in strained Si layers as a function of strain is presented. It includes the effect of strain-induced splitting of the conduction band valleys in Si, inter-valley scattering, and doping dependence. The dependence of the electron mobility components on the orientation of the underlying SiGe layer is taken into account by performing a transformation of the strain tensor from the interface coordinate system to the principal coordinate system. In order to validate the model, Monte Carlo simulations were performed and the results obtained have been fit to experimental data which are available mainly in the form of piezo-resistance coefficients. Results obtained from the model exhibit very good agreement with the Monte Carlo results for all strain levels and substrate orientations. The model is suitable for implementation into any conventional TCAD simulation tool.

Keywords: strained Si, SiGe, mobility model, inter-valley scattering, Technology CAD

1 INTRODUCTION

With the continuous shrinking of feature sizes down to the nanometer regime it is becoming increasingly difficult to obtain performance improvements for CMOS transistors. New materials exhibiting beneficial transport properties are being sought to overcome this problem. In this context the employment of strained Si layers is being strongly considered as an alternative to unstrained Si channels.

The design and optimization of strained Si based device structures necessitates the modeling of carrier mobilities in these devices. We present a model describing the mobility tensor for electrons in strained Si layers as a function of strain. One of the main features of our model is the treatment of inter-valley scattering. Results obtained from the model show very good agreement with the Monte Carlo simulations.

2 STRAIN EFFECTS

Conventionally, strained Si layers are achieved by growth on SiGe buffers. Recently other methods for generating strain in Si have also been proposed [1] [2]. Due

to the lattice mismatch, a pseudomorphically grown Si layer (thickness below critical value) on a relaxed SiGe buffer experiences a biaxial tensile strain. This strain alters the band structure by lifting the degeneracy in both the conduction and valence bands. In the conduction band, the 6-fold degenerate Δ_6 -valleys in Si are found along the $\langle 100 \rangle$ directions at about 80% from the Γ point to the X point. Biaxial tensile strain splits the Δ_6 -valleys into 2-fold degenerate Δ_2 valleys (lower in energy) and 4-fold degenerate Δ_4 valleys (higher in energy). This splitting results in two profitable outcomes. Firstly, the inter-valley phonon scattering is reduced due to decreased number of final available states. Secondly, due to the lower energy of the Δ_2 valleys, the electrons prefer to occupy this valley and therefore experience a lower in-plane effective mass. Both these effects lead to the enhancement of electron mobility.

3 MODELING

As suggested in [3], the anisotropic electron mobility in strained Si/SiGe can be computed by taking the weighted average of the unstrained electron mobility tensor, $\hat{\mu}_{n,uns}^{(i)}$ with the corresponding electron concentration, $n_{str}^{(i)}$ in the i^{th} pair of valley in strained Si,

$$\hat{\mu}_n^{tot} = \sum_{i=1}^3 p^{(i)} \cdot \hat{\mu}_{n,uns}^{(i)}, \quad p^{(i)} = \frac{n_{str}^{(i)}}{\sum_{i=1}^3 n_{str}^{(i)}} \quad (1)$$

$$n_{str}^{(i)} = N_C^{(i)} \cdot \exp \left[\frac{\Delta E_C^{(i)}(y)}{k_B T} \right] \quad (2)$$

Here $n_{str}^{(i)}$ is calculated for non-degenerate doping concentrations, using Boltzmann statistics with $N_C^{(i)}$ as the effective density of states and $\Delta E_C^{(i)}(y)$ the energy shift, for the i^{th} valley. The shifts in energy of the conduction band valleys are given as [4]

$$\Delta E_C^{(i)} = \Xi_d (\varepsilon_{xx} + \varepsilon_{yy} + \varepsilon_{zz}) + \Xi_u \varepsilon_{ii}, \quad i = x, y, z \quad (3)$$

with Ξ_d and Ξ_u as the dilatation and shear deformation potentials for the conduction band. The ε_{ii} 's are the diagonal components of the strain tensor expressed

in the principal coordinate system. Note that (3) holds for arbitrary stress/strain conditions, including uniaxial/biaxial strain.

The model suggested in [3], however, does not consider the change in inter-valley scattering with energy splitting. Thereby it delivers higher values of unstrained mobility for fixed saturation mobility values, see Fig. 1. To overcome this problem, we model the inter-valley

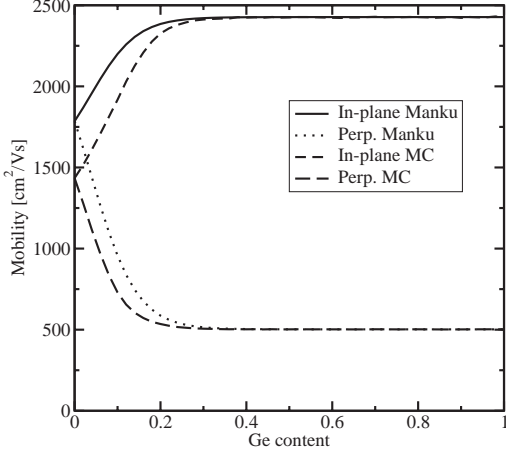


Figure 1: In-plane and perpendicular electron mobilities in strained Si versus the Ge content in SiGe [001] buffer layer calculated using [1]

scattering rate and write the total mobility as in (1) but with $\hat{\mu}_{n,uns}^{(i)}$ replaced by $\hat{\mu}_{n,str}^{(i)}$. Here $\hat{\mu}_{n,str}^{(i)}$ denotes the electron mobility tensors for strained Si for [100], [010], and [001] X-valleys corresponding to directions x , y , and z , respectively.

$$\hat{\mu}_{n,str}^{(i)} = \mu \cdot \hat{m}_{(i)}^{-1}, \quad i = x, y, z \quad (4)$$

$$\hat{m}_x^{-1} = \begin{pmatrix} \frac{m_c}{m_l} & 0 & 0 \\ 0 & \frac{m_c}{m_t} & 0 \\ 0 & 0 & \frac{m_c}{m_t} \end{pmatrix} \quad (5)$$

$$\hat{m}_y^{-1} = \begin{pmatrix} \frac{m_c}{m_t} & 0 & 0 \\ 0 & \frac{m_c}{m_l} & 0 \\ 0 & 0 & \frac{m_c}{m_t} \end{pmatrix} \quad (6)$$

$$\hat{m}_z^{-1} = \begin{pmatrix} \frac{m_c}{m_t} & 0 & 0 \\ 0 & \frac{m_c}{m_t} & 0 \\ 0 & 0 & \frac{m_c}{m_l} \end{pmatrix} \quad (7)$$

The scalar mobility, μ includes the dependence on the energies $\Delta E_C^{(i)}$ and the doping concentration N_I in the strained Si layer.

$$\mu(N_I, \Delta E_C^{(i)}) = \frac{q}{m_c \left(\frac{1}{\tau_{equiv}} + \frac{1}{\tau_{neq}(\Delta E_C^{(i)})} + \frac{1}{\tau_I(N_I)} \right)} \quad (8)$$

In (8) τ_{equiv} denotes the momentum relaxation time due to acoustic intra-valley scattering and inter-valley scattering between equivalent valleys (g -type), $\tau_{neq}(\Delta E_C^{(i)})$ for inter-valley scattering between non-equivalent valleys (f -type scattering), and $\tau_I(N_I)$ for impurity scattering. The effect of the different scattering mechanisms on the total mobility is estimated by Matthiessen's rule in (8). The tensors in (4) are the inverse effective mass tensors with m_t , m_l denoting the transversal and lateral masses for the ellipsoidal X-valleys in Si, scaled to a dimensionless form by the conductivity effective mass, m_c .

$$m_c = \frac{3}{\frac{2}{m_t} + \frac{1}{m_l}} \quad (9)$$

The inter-valley scattering rate is a function of the strain-induced splitting of the valleys and is expressed by a dimensionless factor $h^{(i)}$.

$$h^{(i)} = \frac{\tau_{neq}^0}{\tau_{neq}^{(i)}} = \frac{g(\Delta_{ij}^{em}) + g(\Delta_{il}^{em}) + e^{W_{op}} [g(\Delta_{ij}^{ab}) + g(\Delta_{il}^{ab})]}{2[g(-W_{op}) + \Gamma(\frac{3}{2})]} \quad (10)$$

$$\Delta_{ij}^{em} = \frac{\Delta E_C^{(j)} - \Delta E_C^{(i)}}{k_B T} - W_{op} \quad (11)$$

$$\Delta_{ij}^{ab} = \frac{\Delta E_C^{(j)} - \Delta E_C^{(i)}}{k_B T} + W_{op} \quad (12)$$

$$W_{op} = \frac{\hbar\omega_{opt}}{k_B T} \quad (13)$$

The function g is defined as

$$g(z) = \begin{cases} e^{-z} \cdot \Gamma(\frac{3}{2}) & \forall z > 0 \\ e^{-z} \cdot \Gamma(\frac{3}{2}, -z) & \forall z < 0 \end{cases} \quad (14)$$

Here $\hbar\omega_{opt}$ denotes the phonon energy. $\Gamma(\frac{3}{2}) = \frac{\sqrt{\pi}}{2}$ and $\Gamma(\frac{3}{2}, -z)$ denotes the incomplete Gamma function. (10) describes the total inter-valley scattering rate for electrons to scatter from an initial valley i to final valleys j and l . Replacing the inter-valley term in (8) by (10), the electron mobility for the i^{th} valley in strained Si can

be written as

$$\hat{\mu}_{n,\text{str}}^{(i)}(N_I, y) = \mu^L \cdot \hat{m}_{(i)}^{-1} \times \frac{\beta}{1 + (\beta - 1) \cdot h^{(i)}(y) + \beta \cdot \left(\frac{\mu^L}{\mu^{\text{LI}}} - 1 \right)} \quad (15)$$

where $\hat{m}_{(i)}^{-1}$ denotes the scaled effective mass tensor for the i^{th} valley in (4) and $\beta = f \cdot m_t/m_c$. The mobility enhancement factor f is defined as the ratio of the saturation electron mobility in the transversal valleys of strained Si to the unstrained mobility. μ^L and μ^{LI} signify the lattice mobility and the lattice mobility including the effect of impurity scattering, respectively. Equation (15) can be used to calculate the total mobility tensor for electrons in strained Si as a function of doping concentration N_I and strain. The tensor in (15) is given in the principal coordinate system and has a diagonal form.

4 DISCUSSION

Monte Carlo simulations were performed to validate the model and the results obtained were fit to experimental data, available in the form of piezo-resistance coefficients. For low strain levels the increase in the in-plane electron mobility is linear, characterized by the piezo resistance coefficients. Changing the shear deformation potential Ξ_u from 9.29 eV [5] to 7.3 eV gives good agreement for low strain.

The existing transport models exhibit a considerable quantitative difference in the maximum increase of the in-plane electron mobility in biaxially-strained Si layers when compared to conventional Si. Enhancement values ranging from 56 % [6] up to 180% [7] have been simulated while measurements indicate a value of around 97% [8]. We have adopted a somewhat conservative value of 70% for the enhancement factor, in-between other reported values [9] [10].

The dependence of the electron mobility components on the orientation of the underlying SiGe layer is taken into account by performing a transformation of the strain tensor from the interface coordinate system to the principal coordinate system [11]. Fig. 2 and Fig. 3 show the electron lattice mobility components for different strain levels obtained using (15) for substrate orientations [001] and [110] respectively. As can be seen in Fig. 2, for substrate orientation [001] the two in-plane components of electron mobility are equal with the maximum mobility saturating to a value above 2400 cm²/Vs at about 30% Ge content. For [110] orientation (see Fig. 3) the MC simulation results demonstrate that one of the in-plane components of the electron mobility is equal to the perpendicular component. This feature is also reproduced by the analytical model.

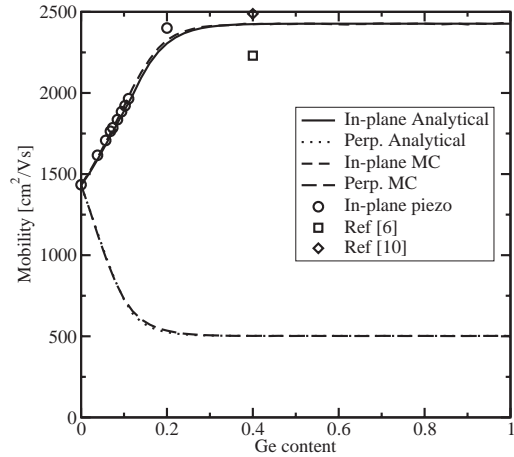


Figure 2: In-plane and perpendicular electron mobilities in undoped strained Si versus the Ge content in the SiGe [001] buffer layer .

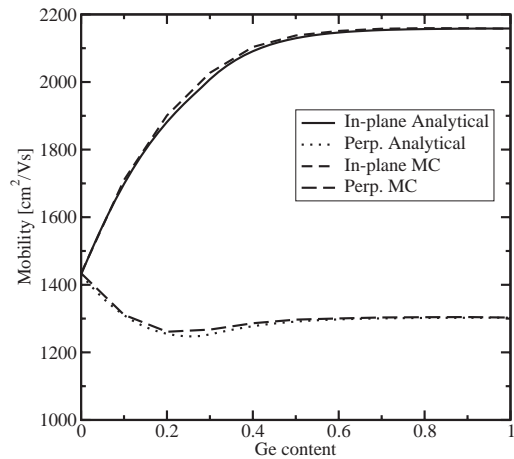


Figure 3: In-plane and perpendicular electron mobilities in undoped strained Si versus the Ge content in the SiGe [110] buffer layer .

The dependence of the in-plane electron mobility in strained Si on the in-plane angle γ can be obtained by taking the projection of the mobility tensor, $\hat{\mu}_n^{\text{tot}}(N_I, y)$ in the direction of in-plane vectors, \vec{a} as,

$$\mu(\gamma) = \vec{a}^T(\gamma) \cdot \hat{\mu}_n^{\text{tot}}(N_I, y) \cdot \vec{a}(\gamma) \quad (16)$$

Fig. 4 shows the variation of the mobility as a function of the angle γ for orientations [110] and [123] of the Si_{0.7}Ge_{0.3} substrate, calculated using (16).

The doping and material composition dependences of the in-plane and perpendicular electron mobilities in strained Si is calculated using (15) with the doping dependence of μ^{LI} for minority and majority electrons in Si given by [12]. Figures 5 and 6 show the dop-

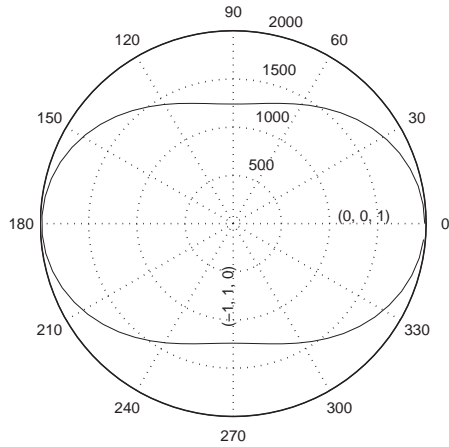


Figure 4: In-plane electron mobilities (in cm^2/Vs) in strained Si versus γ on $\text{Si}_{0.7}\text{Ge}_{0.3}$ [110] buffer layer.

ing dependence of the in-plane minority and majority electron mobility components in strained Si layers for different Ge content in the underlying SiGe for [001] orientation of the substrate. The solid lines depict the results as obtained from the analytical model (15), while the symbols indicate the MC simulation results. As can be seen, the model reproduces the slight increase in minority electron mobility for high doping concentrations for all strain levels, when compared to majority electron mobility.

5 CONCLUSIONS

An analytical model describing the anisotropy of the electron mobility in strained Si has been developed. Results obtained from the model show excellent agreement with MC simulations.

ACKNOWLEDGEMENTS

The authors would like to acknowledge the support from Semiconductor Research Corporation (SRC), project number 998.001.

REFERENCES

- [1] S. Ito *et al.*, in *IEDM Tech.Dig.* (2000), pp. 247–251.
- [2] A. Shimizu *et al.*, in *IEDM Tech.Dig.* (2001), pp. 433–437.
- [3] T. Manku and A. Nathan, *IEEE Trans.Electron Devices* **39**, 2082 (1992).
- [4] I. Balslev, *Physical Review* **143**, 636 (1966).
- [5] M. Rieger and P. Vogl, *Phys.Rev.B* **48**, 14276 (1993).
- [6] F. Bufler, P. Graf, S. Keith, and B. Meinerzhagen, *Appl.Phys.Lett.* **70**, 2144 (1997).

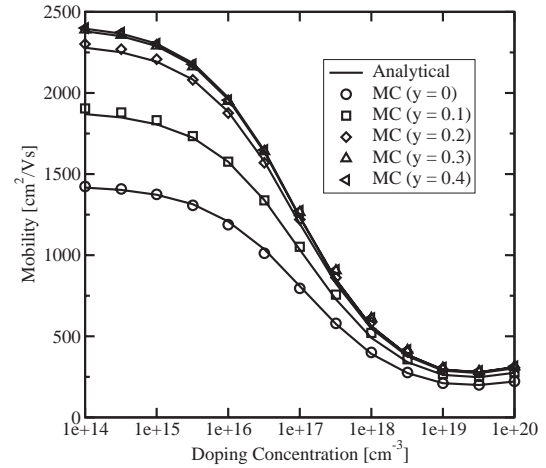


Figure 5: Doping dependence of in-plane electron (minority) mobility in strained Si calculated using (15) for different Ge content in the SiGe [001] substrate.

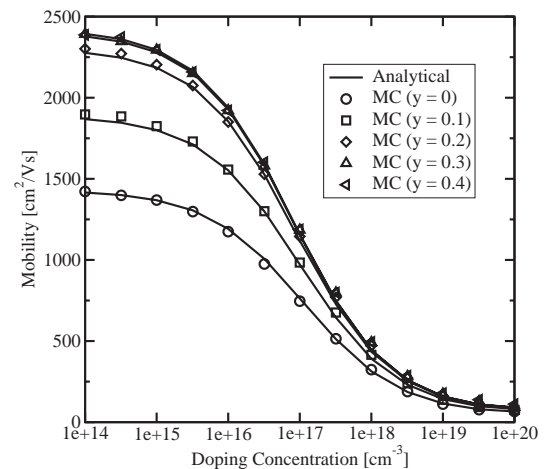


Figure 6: Doping dependence of in-plane electron (majority) mobility in strained Si calculated using (15) for different Ge content in the SiGe [001] substrate.

- [7] T. Yamada, J. Zhou, H. Miyata, and D. Ferry, *IEEE Trans.Electron Devices* **41**, 1513 (1994).
- [8] K. Ismail, S. Nelson, J. Chu, and B. Meyerson, *Appl.Phys.Lett.* **63**, 660 (1993).
- [9] M. Fischetti and S. Laux, *J.Appl.Phys.* **80**, 2234 (1996).
- [10] T. Vogelsang and K. Hofmann, *Appl.Phys.Lett.* **63**, 186 (1993).
- [11] S. Smirnov and H. Kosina, *Solid State Electronics* **48**, 1325 (2004).
- [12] V. Palankovski and R. Quay, *Analysis and Simulation of Heterostructure Devices* (Springer, Wien, New York, 2004).